Sci. Bull.
DOI 10.1007/s11434-015-0828-6

www.scibull.com
www.springer.com/scp

Review

Earth Sciences

Continental crust formation at arcs, the arclogite "delamination" cycle, and one origin for fertile melting anomalies in the mantle

Cin-Ty A. Lee · Don L. Anderson

Received: 9 February 2015 / Accepted: 27 April 2015

Abstract The total magmatic output in modern arcs, where continental crust is now being formed, is believed to derive from melting of the mantle wedge and is largely basaltic. Globally averaged continental crust, however, has an andesitic bulk composition and is hence too silicic to have been derived directly from the mantle. It is well known that one way this imbalance can be reconciled is if the parental basalt differentiates into a mafic garnet pyroxenitic residue/cumulate ("arclogite") and a complementary silicic melt, the former foundering or delaminating into the mantle due to its high densities and the latter remaining as the crust. Using the Sierra Nevada batholith in California as a case study, the composition of mature continental arc crust is shown in part to be the product of a cyclic process beginning with the growth of an arclogite layer followed by delamination of this layer and post-delamination basaltic underplating/recharge into what remains of the continental crust. A model is presented, wherein continuous arc magmatism and production of arclogites in continental arcs are periodically punctuated by a delamination event and an associated magmatic pulse every ~10–30 My. The recycling flux of arclogites is estimated to be ~5 %–20 % that of oceanic crust recycling by subduction. Delaminated arclogites have the necessary trace-element compositions to yield time-integrated isotopic compositions similar to those inferred to exist as reservoirs in the mantle. Because of their low melting temperatures, such pyroxenites may be preferentially melted, possibly forming a component of some hotspot magmas.

Keywords Pyroxenite · Eclogite · Delamination · Cumulate · Continental crust

1 Introduction

Delamination (used loosely here to describe any foundering or detachment) of lower crust or lithospheric mantle due to compositionally or thermally induced densifications has been suggested to explain a number of geologic observations, such as short-lived uplifts, high heat flow and magmatism, and unusual seismic anomalies [1–12]. Such features as uplift and high heat flow are the predicted consequences of having hot asthenospheric mantle upwell passively to replace the "void" created by removal of the deep lithosphere or lower crust. These features have been observed in a number of areas and are increasingly being taken as indirect evidence for recent delamination [11, 13]. If delamination is a general phenomenon, it should be an important means of recycling lower crust or lithospheric mantle back into the Earth's interior, and hence should have an important influence on the compositional evolution of continental crust and the introduction of compositional heterogeneities into the mantle [5, 9, 14]. For example, it has been hypothesized that the felsic composition of continental crust may be the result of preferential removal of mafic lower crust by delamination [4, 9, 11, 15–30]. It has also been hypothesized that this delaminated mafic reservoir may partly contribute to the source regions of midplate and ridge magmas [26, 31].

Don L. Anderson—Deceased

C.-T. A. Lee (✉)
Department of Earth Science, MS-126, Rice University, Houston, TX 77005, USA
e-mail: ctlee@rice.edu

D. L. Anderson
Department of Geological and Planetary Sciences, California Institute of Technology, Pasadena, CA 91125, USA

There are, however, two endmember ways of generating mafic lower crust. One way is via partial melting of basaltic crust during hot subduction or continental collisions, resulting in the generation of mafic restites that may eventually founder back into the mantle [27, 32–38]. Another way is by crystal fractionation of a basalt, generating mafic cumulates at depth in subduction zone volcanoes [4, 11, 18–23, 29, 30, 39–42]. The purpose of this paper is not to debate the mechanisms by which continental crust is formed. Instead, we focus solely on arc magmatism and evaluate whether delamination of mafic lower crust in arcs is an important geologic process in the evolution of arc crust and the generation of fertile melting heterogeneities within the mantle.

2 Delamination in continental arcs

2.1 Garnet pyroxenites and their hypothesized delamination

The difficulty in testing the delamination–crust formation hypothesis is that, if it is correct, some of the evidence for delamination is missing, that is, the putative delaminated material has already been disposed of and is presently lying somewhere hidden in the Earth's interior. However, one place where we have been afforded samples of mafic lower crust prior to delamination is in the Sierra Nevada, the eroded remnant of a Mesozoic arc batholith in California [11, 18]. Small-volume basaltic eruptions in the late Miocene (8 Ma) harbor fragments (xenoliths) of a deep and cold mafic garnet pyroxenitic root, while Pleistocene eruptions contain fragments of hot asthenospheric mantle at equivalent depths [11]. This suggests that a thick, cold mafic root existed beneath the central and eastern Sierras up until the late Miocene, but that sometime in the Pliocene was removed wholesale and replaced by asthenospheric mantle [11, 43]. This interpretation is broadly consistent with the observation that, although the highest elevations in the Sierra Nevada are in the east, the underlying crust is thinnest in this region, which implies that the high elevations are supported by hot (hence low density) asthenospheric mantle [10]. Late Pliocene flare-ups of small-volume basaltic magmatism in the central Sierra might even be the manifestation of post-delamination magmatism [44, 45]. Finally, hypothetical delamination in the central and eastern Sierra during the Pliocene may have even propagated westward as evidenced by high seismic velocity anomalies at depth beneath the western edge of the Sierra Nevada; these have been interpreted to represent ongoing convective downwellings of lower crust or lithospheric mantle [13].

2.2 The relationship between garnet pyroxenites and Sierran mafic to intermediate plutons

Regardless of whether delamination occurred, it is natural to speculate whether the Sierran garnet pyroxenites are complementary to the Sierran batholith. Ducea and Saleeby [29, 30] showed that the Sierran garnet pyroxenites are isotopically similar to the Sierran granitoids and that their major element compositions are roughly complementary. Their observations hint at a petrogenetic relationship with the Sierran granitoids, but the exact nature of the link was not clear. The link can be clarified by considering here a more comprehensive database of Sierran garnet pyroxenites and Sierran granitoids [18]. The Sierran garnet pyroxenites can be divided into two groups, a high MgO (MgO >13 wt%) and a low MgO group (<13 wt%) as shown in Fig. 1a. The former is characterized by high pyroxene to garnet ratios, high Mg# (molar Mg/(Mg + Fe)), high Ni and Cr contents, and low Al_2O_3

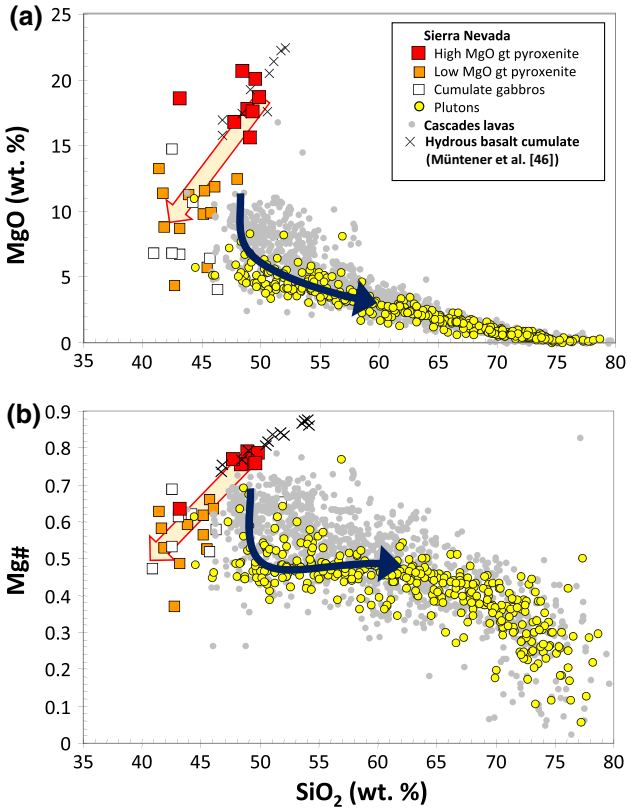

Fig. 1 MgO (**a**), Mg# (**b**) versus SiO_2 in Sierran garnet pyroxenites, Sierran and Peninsular Ranges Batholith plutons, and Cascades volcanics, simplified from Lee et al. [18]. Mg# represents molar Mg/(Mg + Fe_T), where Fe_T represents total iron. Red outlined arrow represents crystal line of descent, and dark blue arrow represents liquid line of descent. Differentiation at relatively constant Mg# requires precipitation of Fe-bearing phases, such as magnetite, and/or basaltic recharge. X symbols refer to experimentally determined cumulates from a hydrous basalt from Müntener et al. [46]

contents, while the latter is characterized by low pyroxene to garnet ratios, low SiO_2, lower Mg#s, low Ni and Cr contents, higher Al_2O_3 contents and higher heavy rare earth element (HREE) abundances [18] (Figs. 1b, 2a).

An equally important observation is that the Sierran mafic to intermediate magmas have high Al_2O_3 (not shown) and low MgO and Mg# (Fig. 1) for a given SiO_2 content compared to basaltic magmas from mid-ocean ridges or young arcs, such as the Cascades. For example, at SiO_2 contents of 50 wt% (typical for basalt), Sierran magma MgO contents are anomalously low, requiring an initial decrease in MgO at constant SiO_2 (Fig. 1a). While the basaltic differentiation trend seen in the Cascades data set can be easily explained by olivine-dominated crystallization, the low MgO and high Al_2O_3 of the Sierran mafic plutons cannot. Instead, the mafic to intermediate leg of the Sierran magmatic differentiation series requires the initial removal of pyroxene-rich residues/cumulates (to drive MgO down at near constant SiO_2) followed by removal of SiO_2-poor or pyroxene-poor residues/cumulates (to drive low MgO magmas toward higher SiO_2). It can be seen that these hypothesized residue/cumulate compositions are matched by the Sierran high and low MgO garnet pyroxenite compositions. These observations corroborate the petrogenetic link between Sierran garnet pyroxenites and the Sierran mafic to intermediate plutons. To distinguish these garnet pyroxenites from true eclogites, which have omphacitic pyroxene, we refer to them as arclogites, a term first suggested by Anderson [47].

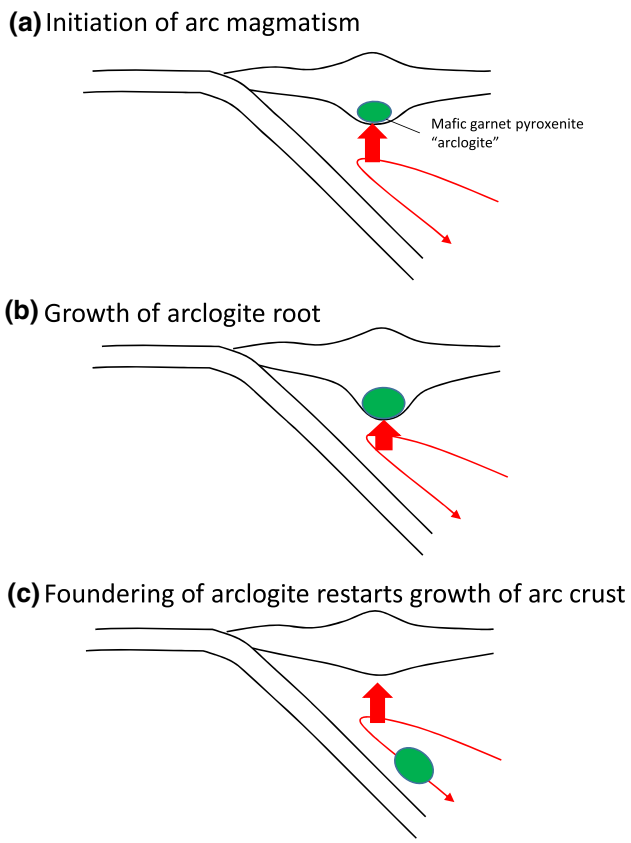

Fig. 2 (Color online) Cartoon showing how arc crust magmatically thickens. In **a,** subduction drives corner flow in the mantle wedge (red line), leading to decompression melting (large red arrow). These melts rise and intrude or underplate the over-riding plate, causing the crust and associated deep crustal mafic cumulate pyroxenites (green) to thicken (**b**). Dense pyroxenite layer eventually reaches a critical thickness after which it founders into the mantle wedge (**c**). Continued melting in the mantle wedge, provided subduction continues, re-initiates the cycle of arc crust growth

2.3 A cumulate origin for Sierran garnet pyroxenites

The origin of the Sierran garnet pyroxenites can be clarified further. The high MgO pyroxenites are not likely to be melt residues because their MgO contents are much too high and would require that they be the residues of >90 % melt extraction [48, 49]. In addition, should the high MgO pyroxenites be the products of melting preexisting basalt, a continuous spectrum of residue compositions would be expected, yet no continuous compositional spectrum is seen in the pyroxenites. The low MgO pyroxenites also cannot represent residues of re-melting primitive basaltic compositions: Melting of eclogitized basalt results in residues with higher MgO and lower SiO_2 [48, 49], but the low MgO pyroxenites have MgO contents lower than any hypothetical primitive mantle-derived basalt. Thus, the low MgO pyroxenites are likely cumulates of evolved basalt that has already crystallized high MgO-type pyroxenites. This genetic relationship between the two pyroxenite groups is also supported by the fact that Mg#, Ni and Cr contents decrease going from high to low MgO pyroxenites [18]. Interestingly, the low MgO pyroxenites have major element compositions very similar to those of Sierran gabbros, which show unequivocal cumulate textures [50]. The Sierran garnet pyroxenites likely crystallized at high pressures (and possibly wet conditions [46]) in order to preferentially crystallize pyroxene instead of olivine (Fig. 1). If so, the Sierran garnet pyroxenites may represent a semi-continuous series of cumulates that is complementary to the fractionation trend seen in mafic to intermediate (50 wt%–60 wt% SiO_2) Sierran magmas (more silicic plutons, such as granites, are unrelated to these pyroxenites). These interpretations are consistent with those based on modeling of Kohistan pyroxenites and felsic rocks [20, 22].

2.4 The need for magmatic recharge

One feature that cannot be explained by fractional crystallization alone is the observation that once the MgO content and Mg# of the Sierran parental magmas have dropped as a consequence of crystallizing high MgO

pyroxenites, the Mg# remains relatively constant with increasing SiO_2 despite our suggestion that this differentiation trajectory is controlled by crystallization of low MgO pyroxenites. Low MgO pyroxenites have higher Mg#s than most of the Sierran plutonic compositions, and thus, fractional crystallization should decrease magmatic Mg#. The constancy of Mg# in the mafic to intermediate spectrum of Sierran plutons indicates that Mg# is buffered (Fig. 1b). One possibility is that this is due to the fractionation of more Fe-rich minerals, such as garnet or cumulate assemblages containing magnetite, giving rise to the well-known calc-alkaline differentiation trend seen in subduction zone magmas [51]. Another explanation, not necessarily exclusive, is that fractional crystallization of garnet pyroxenites is accompanied or followed by basaltic recharge of the residual magma in the form of simultaneous crystallization and recharge of a magma chamber and/or by incremental magmatic underplating/mixing with the lower crust after each magmatic differentiation event [18, 52].

3 The arclogite delamination cycle in continental arcs

Based on the above discussion, garnet pyroxenite accumulation may be a fundamental process in the formation of mature continental arcs, that is, arcs built on preexisting continental lithosphere. In such cases, mantle wedge-derived magmas must pass through a thicker lithosphere and therefore are likely to begin crystallization at greater depths than what might be seen beneath island arcs or young, incipient continental arcs (e.g., the Cascades). The higher pressures of crystallization will favor the precipitation of pyroxenes over olivine.

We propose the following model for the formation and evolution of mature continental arcs (Fig. 2). Our model is constructed to satisfy (1) the dominantly cumulate origin of Sierran garnet pyroxenites, (2) the need for basaltic recharge/underplating, and (3) the possibility that the garnet pyroxenites have delaminated. Thus, as an arc matures, a garnet pyroxenite layer begins to build up at its base due to the progressively thicker lithosphere through which arc magmas must pass (Fig. 2b). Given a continuous background magmatic flux imparted by subduction-induced decompression melting in the mantle wedge [53], the garnet pyroxenite layer thickens gradually with time [4, 18, 54]. Due to the high densities of the garnet pyroxenite cumulates compared to typical peridotitic mantle (Fig. 3; [55]), the garnet pyroxenite layer will eventually founder/delaminate once a critical thickness is reached (Fig. 2c). Hot, asthenospheric mantle should then rise passively to fill the void generated by delamination and, in so doing, generate a pulse of magmatism superimposed on the background flux of melting associated with decompression in the mantle wedge. This renewed melting results in basaltic underplating of the more felsic crust. Some of the basalt will mix with and heat up the base of the overlying continental crust, causing it to melt and generate more evolved magmas, while some basalt will simply crystallize to form more garnet pyroxenite cumulates. If subduction-related magmatism continues, the cycle of growing a cumulate layer followed by delamination will reinitiate. In this way, Sierran magmas can evolve to intermediate compositions without a significant change in Mg# (apart from the initial decrease associated with crystallization of olivine-bearing lithologies and high MgO pyroxenites).

In Fig. 4, we plot the compositions of Sierran pyroxenites, felsic plutons and estimates of the composition of the continental crust relative to mid-ocean ridge basalt (MORB). It can be seen in Fig. 4a that Sierran felsic plutons and the global bulk continental crust, including the present-day global lower continental crust, are depleted in CaO, FeO and MgO relative to basalt. Cumulates with high CaO, FeO and MgO are needed for mass balance, but the present-day lower continental crust clearly does not have the appropriate composition. Arc pyroxenite cumulates, as can be seen from Fig. 4b, have the desired complementary composition. In summary, these qualitative mass balance considerations indicate that the formation of felsic magmatic arcs must in general be accompanied by a significant return of mafic cumulates back into the mantle.

4 Simple models and predictions

4.1 Estimating cumulate growth rate and delamination flux in arcs

Assuming our conceptual model in Sect. 3 is correct, we are now left with quantifying two parameters: (1) the magnitude of the delamination flux of mafic garnet pyroxenites, and (2) the average periodicity of delamination. The delamination flux can be estimated by first considering a mass balance between the two pyroxenite groups and average Sierran pluton compositions with respect to primitive arc basalt. Based on inversion of major element oxides, we have shown that the Sierran garnet pyroxenites collectively amount to 50 %–70 % by mass of the parental basaltic magma, as shown in Fig. 5 [4]. To convert this number to a cumulate growth rate requires that we know the Sierran magmatic flux during the Mesozoic. Because we do not know this, we assume for simplicity that arc magmatic fluxes are relatively uniform globally, regardless of whether mature continental arcs or island arcs are considered. We can then take 3–9 km^3/year as the average total production rate of magmas in arcs [61, 62], ~51,000 km as the total length of subduction zones [57],

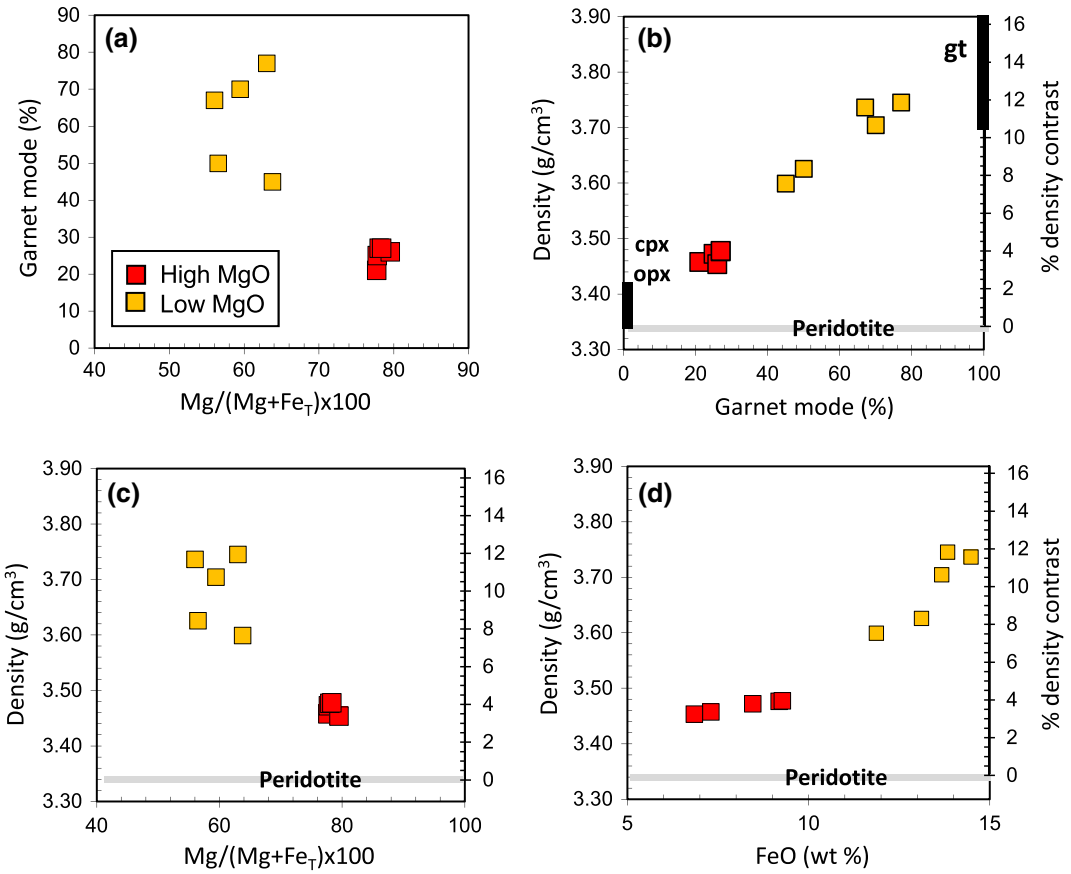

Fig. 3 (Color online) **a** Garnet mode versus Mg# (molar Mg/(Mg + Fe_T) × 100 where Fe_T represents total Fe) in Sierran arc garnet pyroxenites, **b** density in g/cm^3 versus garnet mode, **c** density versus Mg#, **d** density versus bulk FeO (total Fe). Density contrast relative to peridotite is shown on the right-hand *y*-axis (peridotite density taken from Lee [55]). All densities calculated at standard state and pressure (STP) conditions. Figures adapted or using data from Lee et al. [18]

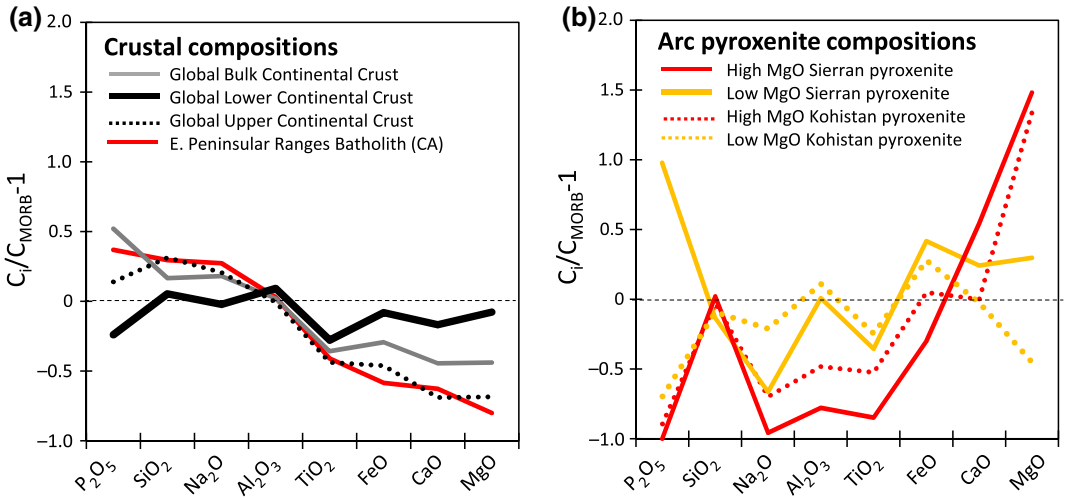

Fig. 4 (Color online) Crustal type (**a**) and arc pyroxenite (**b**) major and minor element compositions using data from Lee [4] and Lee et al. [19] for Sierra Nevada and Jagoutz et al. [20, 22, 39] for Kohistan arc. Average composition of mid-ocean ridge basalt (MORB) is from Arevalo and McDonough [56]. All compositions have been normalized to MORB and represented as relative deviations. Thus, MORB plots at zero, concentrations higher than MORB plot positive and concentrations lower than MORB plot negative. In (**a**) it can be seen that global average lower continental crust cannot balance the composition of the upper continental crust. In (**b**) it can be seen that arc pyroxenites are mafic enough to balance both the composition of the upper continental crust and the bulk continental crust relative to a basaltic parent

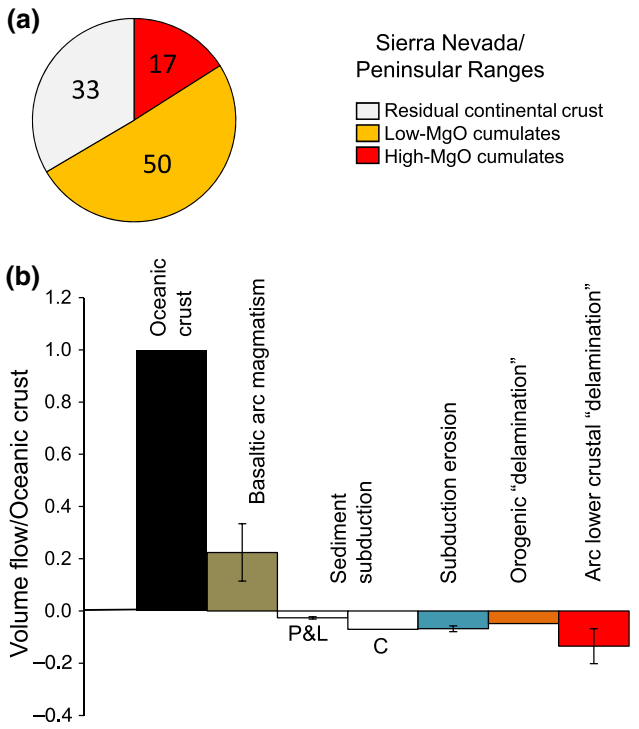

Fig. 5 (Color online) **a** Mass proportions of mafic pyroxenites (low and high MgO) and felsic residual magmas resulting from differentiation of a primary mantle-derived arc basalt. Values are taken from Lee [4] based on inversion of major element compositions, **b** volume flow rates (km^3/year) of various magmatic or sedimentary fluxes, normalized to modern oceanic crust production rates (22.9 km^3/year assuming 7-km-thick crust and areal oceanic crust production rate from Bird [57]). Volume flow rates for arc magmatism, sediment subduction [58, 59], subduction erosion [60], orogenic delamination [58], and arc cumulate delamination [4] are also shown

and ~100 km as the width of magmatic arcs, to arrive at 0.3–1.2 km/My for the average rate of crustal thickening in an arc by magmatic inflation. This corresponds to a cumulate thickening rate ~0.2–0.8 km/My if the mafic cumulates are assumed to be 65 % of the parental magma, as discussed above [4]. Given the higher densities of the pyroxenites compared to felsic plutons and erupted basalts, these numbers might need to be reduced by ~15 %. However, given the uncertainties in all the flux estimates, we do not make this correction in our results. Our estimated arc and delamination fluxes are shown in Fig. 5b normalized to average oceanic crust production rates today (22.6 km^3/My; [57]). Volume flow rates for arc magmatism, sediment subduction [58, 59], subduction erosion [60], orogenic delamination [58], and arc cumulate delamination [4] are also shown for comparison. It can be seen that delamination rates of arc lower crust, while much smaller than the subduction rate of oceanic crust, is comparable if not larger than the amount of sediment being subducted.

4.2 Delamination versus viscous foundering of the pyroxenite layer

We now attempt to predict the periodicity of episodic delamination events by considering how long it takes for the cumulate layer to reach critical negative buoyancy beyond which foundering takes place. The tendency to founder is controlled by the competing effects of negative buoyancy forces (associated with compositional and thermal densification and the thickness of the cumulate layer) and viscous resisting forces. Thermobarometry of Sierran garnet pyroxenites indicates that prior to their hypothesized removal in the Pliocene, they last equilibrated at temperatures below ~800 °C at ~50 km depth [11, 43, 63–66]. This suggests that, following the formation of the cumulate layer, considerable cooling took place, most likely due to impingement upon the cold subducting Farallon plate as the arc root thickened [66].

Using a diabase rheology as an analog for the rheology of garnet pyroxenite [67], we find that the effective viscosity at these temperatures is ~10^{22} Pa s (Table 1; Fig. 6). This is probably a minimum estimate because garnet pyroxenite is probably stronger than diabase. These high viscosities imply that a garnet pyroxenite cumulate layer will be effectively unable to founder viscously even if it is denser than the underlying mantle (Fig. 6). Only at higher temperatures (1,200 °C) can viscous foundering of the pyroxenite layer occur and the problem can be treated as a Rayleigh–Taylor instability [5]. In the case of the Sierra Nevada, the pyroxenite layer is cold and thus too strong to founder viscously, yet all evidence from seismology and temporal changes in xenolith demographics and basalt thermobarometry indicate that the pyroxenite root was removed [11, 44, 45, 68–70].

A dense but effectively rigid cumulate layer can nevertheless be removed if the layer is separated from the overlying crust by a narrow low-viscosity zone, e.g., a weak lower crustal layer. Taking quartz diorite rheology [65] as an analog for the lower part of the more felsic part of the continental crust lying above the garnet pyroxenite layer, a lower crustal weak layer having effective viscosities of ~10^{19} Pa s and a width of roughly 1–5 km is obtained (Fig. 6). This weak zone allows for wholesale removal of the cumulate layer as required by the

Table 1 Flow parameters for some lithospheric materials

	Granite	Wet granite	Diabase	Olivine
A_0 (GPa^{-n}/s)	5	100	3.2×10^6	4×10^{15}
n	3.2	1.9	3.4	3
E_A (kJ/mol)	123	137	260	540

Flow law parameters are taken from [67]

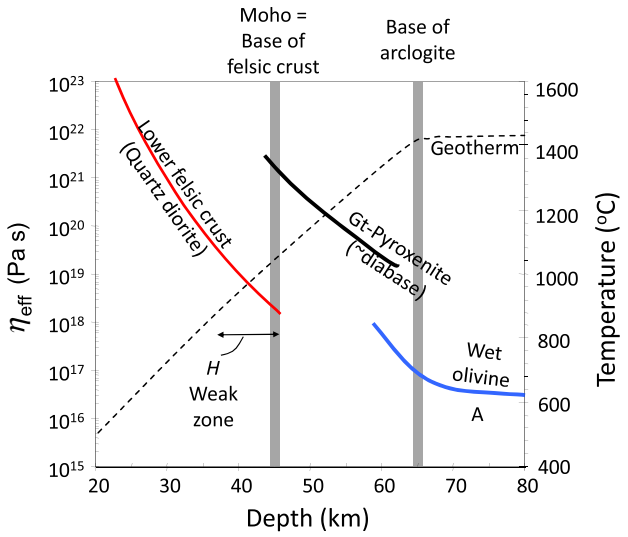

Fig. 6 This figure shows effective viscosities on the *y*-axis versus depth for a hypothetical layered lithosphere (felsic crust, underlain by garnet pyroxenite, e.g., arclogite layer and mantle peridotite). Effective viscosities are calculated using Eq. 3 and the flow laws are shown in Table 1 along a hypothetical geotherm for an arc (dashed line with the right-hand *y*-axis for reference). A background stress state of 0.3 MPa was assumed. Note the presence of a weak lower crustal layer just above the interface between the felsic and mafic (pyroxenite) crust

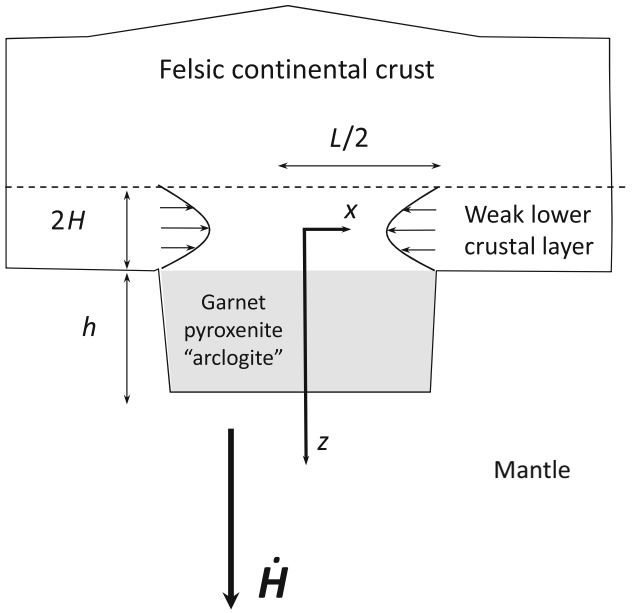

Fig. 7 Highly idealized cartoon of the model for detachment of the pyroxenite (arclogite) layer. The pyroxenite layer is assumed to be separated rheologically from the upper crust by a weak lower crustal layer/gap (Fig. 6). Because the pyroxenite layer is dense, it will tend to sink, resulting in the inward flow of lower crustal material. This lower crustal flow is approximated by laminar flow in the foregoing model

interpretation of xenolith data in the Sierran case study (see Sect. 2.1). This rheological stratification is idealized in Fig. 7 for the purposes of modeling in the next section. Whether or not the dense cumulate layer founders on geologically reasonable timescales will depend on how large the viscous resisting forces are in the weak crustal layer. As the pyroxenite layer sinks, it will suck material into the thin gap, generating a low-pressure region that resists deformation and slows down delamination. The viscous resisting forces in the weak gap will be greatest when the gap is thin. Detachment results in the widening of the gap until viscous resisting forces within the gap become negligible compared with viscous resistance from the underlying asthenospheric mantle.

4.3 Analytical model for delamination

There are a number of sophisticated numerical models describing the detachment of dense mafic lower crust [5, 71–73]. The approach here is to develop simple analytical models in the spirit of Bird [1]. Our main purpose for developing an analytical solution is to make it easier to isolate variables. In particular, we are interested in the case in which the garnet pyroxenite layer can grow with time via magmatic underplating. The basic conceptual approach along with models for simple Newtonian fluids was developed in a pedagogical manner in Lee [4]. Here, we consider the more general case of non-Newtonian rheologies. The model geometry is shown in Fig. 7. Variables and their units are shown in Table 2.

The general flow law for a non-Newtonian rheology is given by

$$\dot{\varepsilon}_{ij} = A\sigma_E^{(n-1)}\sigma_{ij}, \tag{1}$$

where σ_E is the second invariant of the deviatoric stress tensor, A is related to viscosity according to $A = A_0 e^{-E_A/RT}$, R is the gas constant, T is temperature (Kelvin), n is the power-law exponent, A_0 is the preexponential factor with units of G Pa^{-n}/s, and E_A is the activation energy with units of kJ/mol [74, 75]. We ignore the pressure dependence of creep because the variation in lithostatic pressures in our problem is small. Using the following relation

$$\dot{\varepsilon}_E = A\sigma_E^n, \tag{2}$$

the effective viscosity can be determined

$$\eta = A^{-1/n}\dot{\varepsilon}_E^{(1-n)/n}. \tag{3}$$

If the width of the weak or low-viscosity layer H is small compared to the horizontal extent of the cumulate layer L, the motion of the fluid in the thin gap can be approximated as being parallel to the upper and lower boundaries of the gap (e.g., a lubrication approximation is taken). If flow is laminar only in the x direction, the following holds

Table 2 List of parameters and units

	Units	Description
$\dot{\varepsilon}_{zx}$	s^{-1}	Strain rate in direction of x, normal to z
σ_{zx}	Pa	Shear stress
$\dot{\varepsilon}_E$	s^{-1}	Strain rate invariant
σ_E	Pa	Stress invariant
A_0	Pa^{-n}/s	Preexponential factor in flow law
η	Pa s	Effective viscosity
n		Power in flow law
P	Pa	Pressure
Q	m^2/s	Volume flux per unit width
E_A	kJ/mol	Activation energy
t	s	Time
L	m	Length of pyroxenite layer
H	m	Half thickness of low-viscosity layer
H_0	m	Initial half thickness of low-viscosity layer
$\Delta\rho$	kg/m^3	Density contrast
T	°C	Temperature
h	km	Thickness of pyroxenite layer
$\dot{h}$	km/year	Growth rate of pyroxenite layer
v	m/s	Velocity of fluid in slab gap
$\dot{H}$	m/s	Sinking velocity
F	kg/s^2	Force per unit width

$$\dot{\varepsilon}_E = \left[\frac{1}{2}\left(\dot{\varepsilon}_{ij}\dot{\varepsilon}_{ij}\right)\right]^{1/2} = \dot{\varepsilon}_{zx}, \tag{4}$$

where $\dot{\varepsilon}_{zx}$ is the shear strain rate in the horizontal direction x within the weak lower crustal layer. Thus, Eq. 2 becomes

$$\sigma_{zx} = -\frac{1}{A^{1/n}}\dot{\varepsilon}_{zx}^{1/n}, \tag{5}$$

which describes shear stresses in the weak lower crustal layer. We will assume for now that viscous resistance in this lower crustal weak layer is initially much higher than that in the underlying asthenospheric mantle, such that we can approximate the onset of sinking of the pyroxenite layer by considering viscous resistance in the weak layer only. Then, assuming that the lateral pressure gradient in the weak crustal layer is constant, the equations of motion can be integrated to yield

$$\sigma_{zx} = -z\frac{\partial P(x)}{\partial x}. \tag{6}$$

Assuming that driving forces and viscous resistance forces balance (a zero inertia system is assumed), these two equations can be equated and integrated with respect to z to yield an expression for the lateral fluid velocity as a function of gap width H

$$v_x = \frac{A}{n+1}\left(\frac{\partial P}{\partial x}\right)^n\left(z^{n+1} - H^{n+1}\right). \tag{7}$$

Conservation of mass requires that the mass flow of material into the thin gap at every increment in time is balanced by an increase in H in response to the sinking cumulate layer, assuming that the pyroxenite slab is rigid [73]. The volume flux into the gap is

$$Q = \int_{-H}^{H} v_x \mathrm{d}z = 2\int_0^H v_x \mathrm{d}z, \tag{8}$$

which corresponds to

$$Q_{\text{total}} = -2A\left(\frac{\partial P}{\partial x}\right)^n\left[\frac{H^{n+2}}{n+2}\right]. \tag{9}$$

This volume flow must equal

$$Q = -(2\dot{H})(L/2) = -\dot{H}L, \tag{10}$$

where $\dot{H}$ is the sinking velocity of the cumulate layer. Equations 9 and 10 and isolating for $\frac{\partial P}{\partial x}$ yield

$$\frac{\partial P}{\partial x} = \left[\frac{\dot{H}L(n+2)}{2H^{n+2}A}\right]^{1/n}. \tag{11}$$

Integrating with respect to x and applying the boundary condition, $P = P_{L/2}$ when $x = L/2$, yields

$$P_{L/2} - P(x) = \left[\frac{\dot{H}L(n+2)}{2H^{n+2}A}\right]^{1/n}\left(\frac{L}{2} - x\right). \tag{12}$$

The suction force per unit width (in third dimension), F_P, is

$$F_P = \int_0^{L/2}\left(P_{L/2} - P(x)\right)\mathrm{d}x. \tag{13}$$

Integrating (12) yields the total viscous resisting force acting within the weak lower crustal layer

$$F_P = \left[\frac{\dot{H}^{1/n}}{H^{(n+2)/n}}\right]\left[\frac{L(n+2)}{2A}\right]^{1/n}\frac{L^2}{8}. \tag{14}$$

Because our system can be assumed to be a zero inertia system (Reynold's number is zero), the viscous resisting force is balanced exactly by the buoyancy force

$$F_g = (\Delta\rho)(L/2)hg, \tag{15}$$

where $\Delta\rho$ is the density contrast between the pyroxenite layer and the underlying asthenospheric mantle, h is the thickness of the cumulate layer, and g is gravity. Equations 14 and 15 give the sinking rate as a function of gap width

$$\dot{H} = \frac{F_g^n}{K^n}H^{n+2}, \tag{16a}$$

$$K = \left[\frac{L(n+2)}{2A}\right]^{1/n}\frac{L^2}{8}. \tag{16b}$$

Equation 16a shows that the sinking velocity increases with gap width H to the $n+2$ power and therefore increases with time. We can integrate Eq. 16a to get H as a function of time

$$H(t) = \left[\frac{1}{H_0^{n+1}} - \frac{(n+1)F_g^n}{K^n}t\right]^{-1/(n+1)}. \tag{17}$$

For a cumulate layer of thickness h, the critical time for foundering to take place occurs when $H/H_0 \gg 1$ and is expressed as

$$t_{\text{crit}} = \frac{K^n}{F_g^n(n+1)H_0^{n+1}}. \tag{18}$$

We can also define the time at which the gap width increases by twice the initial gap width

$$t_{2H_0} = \frac{K^n}{(n+1)F_g^n}\left(\frac{2^{n+1}-1}{(2H_0)^{n+1}}\right) = \left(1 - \frac{1}{2^{n+1}}\right)t_{\text{crit}}. \tag{19}$$

At times greater than t_{2H_0}, it can be seen that the sinking velocity begins to "accelerate", in which case, we can assume that delamination is well on its way.

In all of the above equations, if n is assumed to be 1, the foregoing simplifies to the equations derived by Lee [4] for Newtonian rheologies. Specifically, the time for delamination for $n = 1$ is

$$t_{\text{crit}} = \frac{3}{16}\frac{\eta}{\Delta\rho g h}\left(\frac{L}{H_0}\right)^2, \tag{20}$$

where η is the effective viscosity ($\eta = 1/A$ for $n = 1$). It can be seen that the time for delamination increases with increasing effective viscosity of the lower crustal layer and increasing aspect ratio of the gap L/H_0 and decreasing density contrast and size of the pyroxenite layer (Fig. 8a). Thus, for $\Delta\rho$ of 500 kg/m^3, h of 30 km, and η between $\sim 10^{19}$ and 10^{21} Pa s, delamination occurs within 100 My for relevant L/H_0. When $n > 1$, as in the case for dislocation creep ($n \sim 3$), the time for delamination will be less than that given for the Newtonian ($n = 1$) regime, assuming all other parameters in the flow law are the same. In Fig. 9, we show delamination time t_{crit} for non-Newtonian rheologies in which dry olivine, dry granite and wet granite make up the low-viscosity layer, assuming the geotherm shown in Fig. 6. Obviously, the layer is not composed of olivine, so this is shown only for comparison. For a dry granite at 600 °C, delamination occurs before 100 My, and for a wet granite rheology, delamination occurs in less than 1 My. Most likely, the rheology of the weak lower crustal layer will be intermediate between a wet and dry granite, and we conclude that delamination of the pyroxenite layer should occur spontaneously on timescales of a few to tens of millions of years.

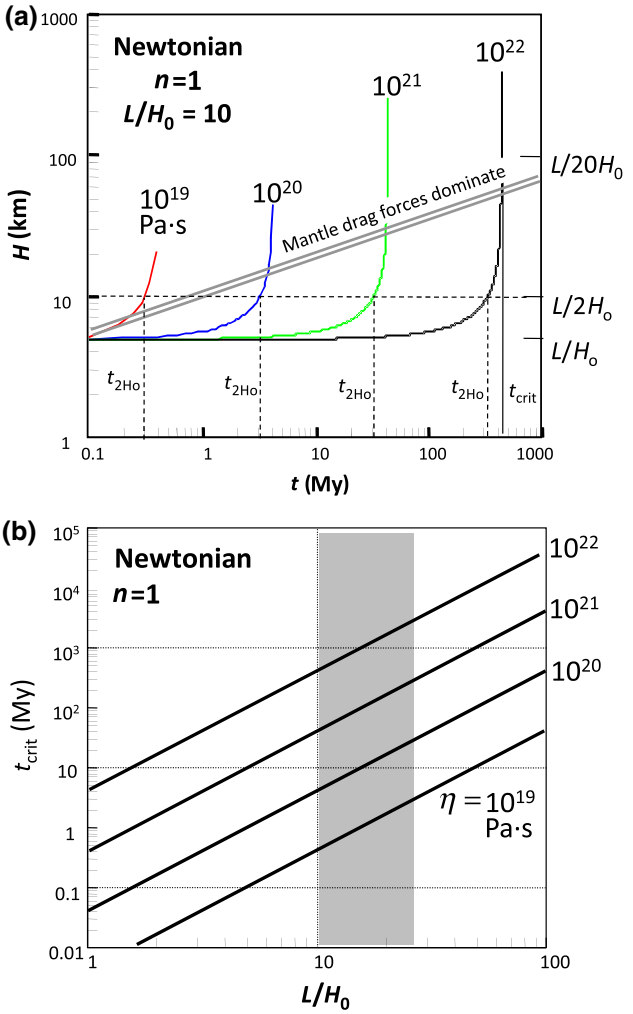

Fig. 8 **a** Delamination, t_{crit}, as a function of L/H_0, showing the dependence of delamination on the aspect ratio of the low-viscosity gap. For the Sierra Nevada, L/H_0 ranges between 10 and 25 (gray vertical bar), **b** one-half of the gap thickness (H) as a function of time (My), where $H_0 = 5$ km, $L = 50$ km, and density contrast between pyroxenite slab and asthenosphere $\Delta\rho = 500$ kg/m^3, pyroxenite layer thickness $h = 30$ km, and a Newtonian rheology ($n = 1$) with viscosities η (=1/A) of 10^{19} to 10^{22} Pa s for the low-viscosity layer. H grows very slowly initially, dropping off exponentially at t_{2H_0} (vertical dashed lines), when $H = 2H_0$ (horizontal dashed line). Delamination time is denoted by t_{crit} (e.g., when H approaches infinite). Diagonal double line represents the point at which asthenospheric mantle viscous resistance to sinking F_A becomes larger than the viscous resistance in the lower crustal weak layer F_P (e.g., when $F_A > F_P$), assuming an asthenospheric viscosity of 10^{21} Pa s. As can be seen, exponential growth of H occurs before F_A becomes important

As noted from the outset, we did not account for the viscous resisting force, F_A, associated with the underlying asthenospheric mantle (this was also ignored by [1]). Accounting for this effect should increase t_{crit}, but by how much? We can estimate the relative contribution of F_A relative to F_P from the relation $\dot{\varepsilon}_{xz} = \dot{H}/L$, where the

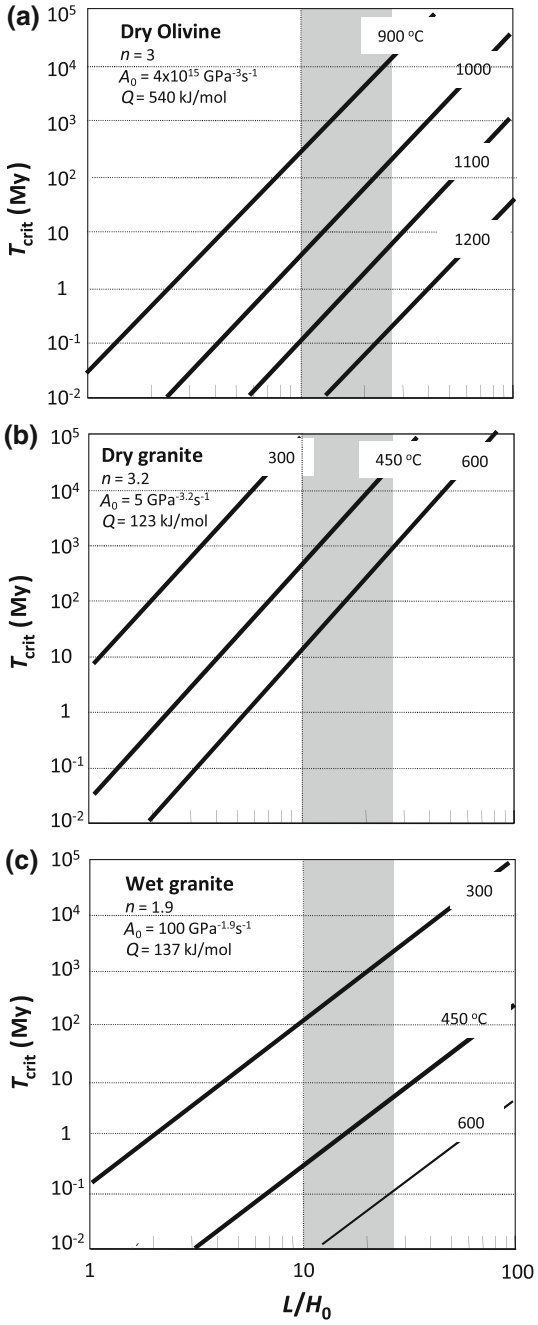

Fig. 9 Effect on t_{crit} for non-Newtonian rheologies. **a** Dry olivine for the asthenospheric mantle, **b** dry granite for the upper crust, **c** wet granite for the upper crust. Vertical gray bar represents the range of L/H_0 relevant to the Sierra Nevada. Rheologic laws are taken from Table 1 [67]. $\Delta\rho = 500$ kg/m^3 and pyroxenite layer thickness $h = 30$ km

deformation imposed on the surrounding asthenosphere by the sinking slab is $\dot{\varepsilon}_{xz}$, the velocity of the sinking slab is $\dot{H}$ (by differentiation of Eq. 9), and the length scale over which deformation in the asthenosphere occurs is taken to scale with the length of the slab, L. For a Newtonian fluid ($n = 1$), the asthenospheric viscous resisting force (per unit width), F_A, is then expressed as:

$$F_A = \sigma_{xz}(h + L/2) = \eta\dot{\varepsilon} = \frac{\dot{H}}{A_A}\frac{h + L/2}{L}, \tag{21}$$

where the stress is taken to act on the surface area exposed to the asthenosphere ($h + (L/2)$) and $1/A_A$ is used to denote the Newtonian viscosity of the asthenospheric mantle, which is not the same as that in the low-viscosity gap A. F_A can be compared to F_P for the case in which $n = 1$:

$$F_P = \frac{\dot{H}}{A}\left(\frac{L}{H}\right)^3\frac{3}{16}, \tag{22}$$

$$\frac{F_P}{F_A} = \frac{3}{16}\frac{A_A}{A}\frac{L}{h + (L/2)}\frac{L^3}{H^3}. \tag{23}$$

Asthenospheric viscous resistance F_A becomes important when $F_P/F_A < 1$. For a given A_A/A, F_P/F_A decreases with $1/H^3$, which is to say that viscous resistance in the gap dominates initially and only after the pyroxenite slab detaches ($H > 2H_0$) does resistance from the asthenospheric mantle become important. In other words, Eqs. 16 and 17 are only valid up until $F_P/F_A = 1$. Assuming parameters relevant for the Sierra Nevada ($L/h = 50$ km/30 km) and the unusual case in which $A_A = A$, we find that $F_P/F_A = 1$ when $H = 30$ km (Fig. 8b).

We note that the viscosity of the lithospheric mantle may also play a role as in the case of destabilization of cratonic mantle [76–82]. In the case of cratonic lithosphere, the lithospheric mantle could be ~200 km thick, whereas the lower crust is less than 20 km thick. In the case of arc lithosphere, it seems likely that the lithospheric mantle is thin, given that mature volcanic arcs may have crustal roots extending down to depths in excess of 60 km [11, 21, 29, 30, 64–66]. Additionally, in juvenile or island arcs, thermobarometric constraints on the origin of basaltic magmas suggest the presence of hot asthenospheric mantle at depths shallower than 60 km [83, 84], leaving little room for lithospheric mantle when typical arc crusts are ~20–30 km thick.

4.4 Application to the general case in which the pyroxenite layer is growing

In the more general case of constant background magmatism, the cumulate layer should be growing by magmatic underplating. If so, h is a function of t, and hence, F_g increases while sinking is taking place. In such a scenario, the above equations are solved incrementally assuming some knowledge of the cumulate growth rate $\dot{h}$, which is some fraction of the total juvenile arc magmatic production rate (Fig. 5). Modeling results are shown in Fig. 10 assuming a temperature of 800 °C in the lower crust, a

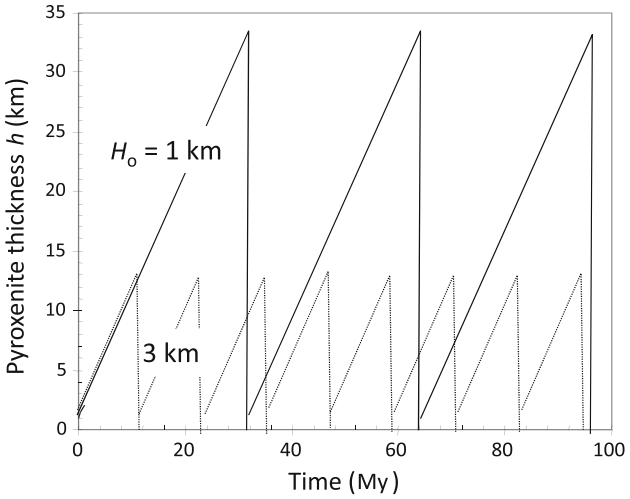

Fig. 10 Pyroxenite layer thickness h grows with time at a rate defined by juvenile arc magmatic flux ($km^3/km^2/My$) as represented by the slope of h versus t. As the dense pyroxenite layer grows, the negative buoyancy driving force increases as h, causing the pyroxenite layer to sink and eventually delaminate. We assume wholesale delamination. After delamination, continual magmatic flux permits the pyroxenite layer to grow again, reinitiating the cycle. Calculations are done for different initial thicknesses of lower crustal weak layer (half widths of 1 and 3 km). $\Delta\rho = 500$ kg/m^3 and a power-law rheology of quartz diorite at 800 °C is assumed

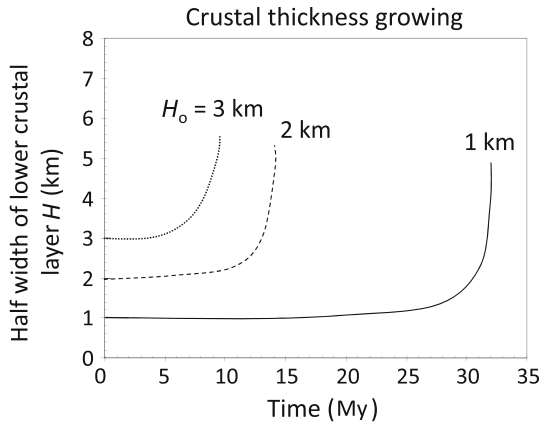

Fig. 11 Detachment rate as a function of time. Same as in Fig. 10 except the effect of initial thickness H_0 of lower crustal weak layer is shown. Crustal thickening rate same as in Fig. 10. $\Delta\rho = 500$ kg/m^3 and a power-law rheology of quartz diorite at 800 °C is assumed

quartz diorite rheology for the weak lower crust, a density contrast of $\sim$500 kg/m^3 based on density estimates for garnet pyroxenites and peridotites [18, 47] (Fig. 3), and a constant cumulate growth rate $\dot{h}$ (the slope of the line in Fig. 10). It can be seen that for a reasonable range in initial gap widths, H_0, it takes 10–30 My for foundering to take place (Fig. 11); the cumulate thickness at the time of foundering ranges between 10 and 35 km (Fig. 10), resulting in large heterogeneities recycled into the mantle at any given time. Once the cumulate layer founders, it is replaced by hot asthenosphere, which undergoes decompression partial melting. This results in a magmatic pulse superimposed on a background magmatic flux associated with flux melting in the mantle wedge.

5 Implications and predictions

5.1 Global implications

In summary, the silicic nature of bulk continental crust can in part be explained by the refinement of basalt at mature continental arcs through a cyclic process of fractional crystallization, delamination, and post-delamination magmatism, all of which are superimposed on a constant baseline magmatic flux associated with flux melting in the mantle wedge. Our conclusions do not rule out other proposed mechanisms for generating felsic continental crust, such as partial melting of subducting oceanic crust or overthickened basaltic crust [16, 17, 32, 34, 35, 38, 85], remelting of sediments [86, 87] or relamination of sediments [88]. Additional work is needed to assess which of these proposed mechanisms dominates the formation of continental crust throughout Earth's history. The immediate prediction of our hypothesis is that continental arc magmatism should be punctuated by magmatic pulses associated with delamination of mafic cumulates, e.g., arclogites. This in turn predicts that continental arcs should be characterized by multiple delamination events. There is some evidence that magmatism in continental arcs, such as the Sierra Nevada, may be episodic [89]. There is also some tentative evidence for multiple delamination events in the Sierra Nevada [43, 90] and the Andes in South America [91]. It is even likely that delamination events in continental arcs are closely coupled with foreland fold-and-thrust belts because removal of arc lower crust and lithospheric mantle provides room for continental basement to be underthrust beneath the arc [92]. Indeed, continental upper plate lithologies have been found at 45 km depth in the Sierran arc, indicating that mafic magmatism and tectonic underthrusting were coeval [93].

In any case, an important implication of our hypothesis is that continental crust formation, at least in continental arcs, is coupled with the recycling of mafic garnet pyroxenites back into the mantle. The question then is how significant is this recycling flux compared to subduction recycling of oceanic crust? Assuming that garnet pyroxenite formation occurs in all arcs and using additional assumptions already outlined in Sect. 4.1, we arrive at a cumulate recycling rate of 1.5–6 km^3/year ([4]), which is not insignificant when compared to the total recycling rate of $\sim$20 km^3/year for oceanic crust (basaltic + gabbroic sections [61]). However, it is not clear whether primary

garnet pyroxenite accumulation occurs in all arcs ([16, 23]). Island arcs and young, incipient continental arcs (e.g., the Cascades) appear not to have a strong garnet pyroxenite signature (compare Cascades data to Sierran data in Fig. 1), indicating that garnet pyroxenite was probably never on the liquidus. The lack of a garnet pyroxenite signature in young arcs and island arcs may stem from the fact that the preexisting lithosphere through which mantle-derived magmas pass is thinner in these regions [94]. Under these conditions, crystallization occurs at lower pressures where olivine is the dominant liquidus phase. If primary garnet pyroxenites only accumulate in continental arcs, then our calculated delamination recycling flux of garnet pyroxenites is a maximum bound. However, it is still possible for garnet pyroxenites to form in island arc environments by the subsolidus conversion of lower pressure cumulates (gabbros) to garnet pyroxenites. Once converted, these metamorphosed cumulates would be dense and could potentially delaminate as well. The only difference would be that garnet pyroxenites in continental arcs are primary cumulates, whereas those in island arcs might be metamorphosed low-pressure cumulates.

Given the possibility that the recycling flux of garnet pyroxenites via delamination might be significant, we end with the question of whether recycled arc-type garnet pyroxenites can be detected, that is, are these pyroxenites ever sampled in hotspots? The Sierran pyroxenites have the following primitive mantle-normalized ratios (denoted with subscript N): $(Sm/Nd)_N \leq 1$, $(Lu/Hf)_N \leq 1$, $(U/Pb)_N$ only slightly greater than 1, and $(Rb/Sr)_N$ ranging between 1 and that for continental crust [18, 19]. In particular, these low U/Pb signatures may also be related to the fact that these garnet pyroxenites contain primary cumulate sulfide [42, 95]. These parent–daughter ratios will lead to time-integrated Nd, Hf, Pb and Sr isotopic compositions similar to the EM1 isotopic component seen in some hotspot magmas [96] and are hence reasonable candidates for certain recycled reservoirs believed to exist in the mantle [26]. Because of the likely lower melting temperatures of both the high MgO and low MgO Sierran garnet pyroxenites [97–100], such pyroxenite blobs could be preferentially melted and reacted with the mantle, forming the source reservoirs of some hotspot magmas [99, 101, 102]. Detecting these heterogeneities in the source regions of intraplate magmas will be aided by systematic study of major element [101, 103] and mildly incompatible element compositions (namely the first-row transition metals) [104–106].

5.2 Implications for Cretaceous to present volcanism in eastern Asia and western North America

There is growing evidence that arc-related pyroxenitic roots were generated beneath much of westernmost North America during the Cretaceous and early Paleogene. Some of these mafic roots may have already foundered (as evidenced by seismic studies indicating hot asthenospheric mantle at depths where pyroxenites were once present based on the xenolith record [10, 11]), but some may still persist [12]. Is it possible that some of the volcanism associated with Basin and Range extension is related to preferential melting of these pyroxenite layers, as suggested long ago by Leeman and Harry [108]? Much work has been placed recently on estimating mantle potential temperatures of intraplate basalts [68, 83] in an attempt to constrain the thickness of the lithosphere and temperature of the asthenosphere. A fundamental step in estimating mantle temperatures from basalts is to back-correct for olivine fractionation until the liquid is in equilibrium with peridotitic mantle. However, if pyroxenites are interleaved with the peridotites, then smaller fractionation corrections are required and estimated temperatures would be lower. There is no easy way to resolve these differences.

In this context, it is useful to turn to the extensive studies of Cretaceous to Neogene basalts in eastern Asia, particularly in northeastern China. Much of eastern Asia was marked by continental arc volcanism in the Jurassic and Cretaceous, much like western North America at the same time [109–111]. Such volcanism must have left behind great thicknesses of mafic pyroxenites at the base of the crust or in the lithospheric mantle throughout much of eastern China. A curious feature of many basalts in eastern China is that they have high total Fe contents, which if one were to fractionate correct to nominal mantle peridotite would yield temperatures 100–200 °C higher than ambient mantle beneath ridges. However, a number of studies have noted that these basalts have unusual Fe/Mn and Zn/Fe systematics, which suggest a pyroxenite-bearing source rather than a pure peridotite source [106, 112–114]. It has been suggested that these pyroxenite-bearing mantle sources could be derived by re-melting of previously delaminated lower crustal pyroxenites (presumably arclogites?) [115, 116]. However, it is also possible that these pyroxenite lithologies may still be within the lithosphere, preferentially melting by extensional decompression if lithospheric thinning occurred by extension or thermal erosion, rather than by delamination (cf. [117–120]). In any case, the unusual transition metal systematics of Cenozoic basalts in eastern China (in the North and South China Blocks) suggest that the mantle melting regime beneath this area is more fertile. Recent work on peridotite xenoliths from the South China block seem to confirm the unusually high fertility of the mantle lithosphere [121]. No such detailed study of transition metal systematics has been conducted for western North American basalts, so it is unclear whether much of the volcanism in the area is driven by thermal variations in the asthenosphere or to the

presence of fertile heterogeneities associated with pyroxenite veins. A promising future direction of research will be to use basalts to interrogate both mantle fertility and temperature beneath eastern Asia and western North America.

6 Conclusions and future directions

In summary, we show that arc magmatism, particularly in continental arcs, generates thick and dense garnet pyroxenite cumulates, which eventually founder back into the mantle. The entire process, from initiating of magmatism to delamination, may take 10–30 My, implying that during the lifespan of a magmatic arc, numerous pulses of cumulate foundering may occur. What we have not yet considered are other processes that modulate the thickness of arc crust, such as erosion and tectonics (shortening and extension). Erosion and tectonics are also affected by magmatic inflation and vice versa, so the full feedbacks must also be considered. Another feedback that we did not consider was the effect of crustal thickening on suppressing the efficiency of decompression melting in the mantle wedge [55], which would influence crustal growth rates. Although our approach is simplistic and nature is complex, it is hoped that simple analytical solutions may provide a means of systematically evaluating each of these feedbacks in future studies.

Acknowledgments This work was supported by NSF (EAR-0309121, 0440033). The models were developed by Lee in 2000 as Chapter 7 of his PhD thesis [122]. In 2005, the paper was revived when D. Anderson was a Wiess Visiting professor at Rice University, but we never finished the paper. After D. Anderson's death in December 2014 and a once in a decade effort to clean his office, Lee stumbled upon this paper again. The resurrected manuscript has been expanded and revised to bring it up to date. We thank H. Stone, M. Manga and R. J. O'Connell for inspiring simplicity.

Conflict of interest The authors declare that they have no conflict of interest.

References

1. Bird P (1979) Continental delamination and the Colorado Plateau. J Geophys Res 84:7561–7571
2. Molnar P, Houseman GA, Conrad CP (1998) Rayleigh–Taylor instability and convective thinning of mechanically thickened lithosphere: effects of non-linear viscosity decreasing exponentially with depth and of horizontal shortening of the layer. Geophys J Int 133:568–584
3. Conrad CP, Molnar P (1997) The growth of Rayleigh–Taylor-type instabilities in the lithosphere for various rheological and density structures. Geophys J Int 129:95–112
4. Lee C-TA (2014) Physics and chemistry of deep continental crust recycling. Treatise Geochem 4:423–456
5. Jull M, Kelemen P (2001) On the conditions for lower crustal convective instability. J Geophys Res 106:6423–6446
6. Houseman G, Neil EA, Kohler MD (2000) Lithospheric instability beneath the Transverse Ranges of California. J Geophys Res 105:16237–16250
7. Houseman GA, McKenzie DP, Molnar P (1981) Convective instability of a thickened boundary layer and its relevance for the thermal evolution of continental convergent belts. J Geophys Res 86:6115–6132
8. Houseman GA, Molnar PA (1997) Gravitational (Rayleigh–Taylor) instability of a layer with non-linear viscosity and convective thinning of continental lithosphere. Geophys J Int 128:125–150
9. Kay RW, Kay SM (1993) Delamination and delamination magmatism. Tectonophysics 219:177–189
10. Wernicke B, Clayton R, Ducea M et al (1996) Origin of high mountains in the continents: the southern Sierra Nevada. Science 271:190–193
11. Ducea MN, Saleeby JB (1996) Buoyancy sources for a large, unrooted mountain range, the Sierra Nevada, California: evidence from xenolith thermobarometry. J Geophys Res 101:8229–8244
12. Levander A, Schmandt B, Miller M et al (2011) Continuing Colorado Plateau uplift by delamination-style convective lithospheric downwelling. Nature 472:461–465
13. Zandt G, Gilbert H, Owens TJ et al (2004) Active foundering of a continental arc root beneath the southern Sierra Nevada in California. Nature 431:41–46
14. Rudnick RL (1995) Making continental crust. Nature 378:571–578
15. Kay RW, Kay SM (1988) Crustal recycling and the Aleutian arc. Geochim Cosmochim Acta 52:1351–1359
16. Kelemen PB, Hanghoj K, Greene AR (2003) One view of the geochemistry of subduction-related magmatic arcs, with an emphasis on primitive andesite and lower crust. Treatise Geochem 3:593–659
17. Kelemen PB (1995) Genesis of high Mg# andesites and the continental crust. Contrib Mineral Petrol 120:1–19
18. Lee C-TA, Cheng X, Horodyskyj U (2006) The development and refinement of continental arcs by primary basaltic magmatism, garnet pyroxenite accumulation, basaltic recharge and delamination: insights from the Sierra Nevada, California. Contrib Mineral Petrol 151:222–242
19. Lee C-TA, Morton DM, Kistler RW et al (2007) Petrology and tectonics of Phanerozoic continent formation: from island arcs to accretion and continental arc magmatism. Earth Planet Sci Lett 263:370–387
20. Jagoutz E, Burg J-P, Hussain S et al (2009) Construction of the granitoid crust of an island arc part I: geochronological and geochemical constraints from the plutonic Kohistant (NW Pakistan). Contrib Mineral Petrol 158:739–755
21. Jagoutz O, Schmidt MW (2012) The formation and bulk composition of modern juvenile continental crust: the Kohistan arc. Chem Geo 298–299:79–96
22. Jagoutz OE (2010) Construction of the granitoid crust of an island arc. Part II: a quantitative petrogenetic model. Contrib Mineral Petrol 160:359–381
23. DeBari SM, Sleep NH (1991) High-Mg, low-Al bulk composition of the Talkeetna island arc, Alaska: implications for primary magmas and the nature of arc crust. Geol Soc Am Bull 103:37–47
24. Gao S, Luo T-C, Zhang B-R et al (1998) Chemical composition of the continental crust as revealed by studies in East China. Geochim Cosmochim Acta 62:1959–1975
25. Gao S, Zhang B, Jin Z et al (1998) How mafic is the lower continental crust? Earth Planet Sci Lett 161:101–117

26. Tatsumi Y (2000) Continental crust formation by crustal delamination in subduction zones and complementary accumulation of the enriched mantle I component in the mantle. Geochem Geophys Geosys 1:2000GC000094
27. Arndt NT, Goldstein SL (1989) An open boundary between lower continental-crust and mantle: its role in crustal formation and recycling. Tectonophysics 161:201–212
28. Herzberg CT, Fyfe WS, Carr MJ (1983) Density constraints on the formation of the continental Moho and crust. Contrib Mineral Petrol 84:1–5
29. Ducea MN (2002) Constraints on the bulk composition and root foundering rates of continental arcs: a California arc perspective. J Geophys Res. doi:10.1029/2001JB000643
30. Ducea MN, Saleeby JB (1998) The age and origin of a thick mafic-ultramafic keel from beneath the Sierra Nevada batholith. Contrib Mineral Petrol 133:169–185
31. McKenzie D, O'Nions RK (1983) Mantle reservoirs and ocean island basalts. Nature 301:229–231
32. Rapp RP, Shimizu N, Norman MD (2003) Growth of early continental crust by partial melting of eclogite. Nature 425:605–609
33. Niu Y, Zhao Z, Zhu D-C et al (2013) Continental collision zones are primary sites for net continental crust growth—a testable hypothesis. Earth-Sci Rev 127:96–110
34. Rollinson HR (1997) Eclogite xenoliths in West African kimberlites as residues from Archaean granitoid crust formation. Nature 389:173–176
35. Rudnick RL, Fountain DM (1995) Nature and composition of the continental crust: a lower crustal perspective. Rev Geophys 33:267–309
36. Barth MG, Rudnick RL, Horn I et al (2002) Geochemistry of xenolithic eclogites from West Africa, part 2: origins of the high MgO eclogites. Geochim Cosmochim Acta 66:4325–4345
37. Barth MG, Rudnick RL, Horn I et al (2001) Geochemistry of xenolithic eclogites from West Africa, Part I: a link between low MgO eclogites and Archean crust formation. Geochim Cosmochim Acta 65:1499–1527
38. Foley SF, Tiepolo M, Vannucci R (2002) Growth of early continental crust controlled by melting of amphibolite in subduction zones. Nature 417:837–840
39. Jagoutz O, Muntener O, Ulmer P et al (2007) Petrology and mineral chemistry of lower crustal intrusions: the Chilas Complex Kohistan (NW Pakistan). J Petrol 48:1895–1953
40. Ducea M (2001) The California arc: thick granitic batholiths, eclogitic residues, lithosphere-scale thrusting, and magmatic flare-ups. GSA Today 11:4–10
41. Lee C-TA, Bachmann O (2014) How important is the role of crystal fractionation in making intermediate magmas? Insights from Zr and P systematics. Earth Planet Sci Lett 393: 266–274
42. Lee C-TA, Luffi P, Chin EJ et al (2012) Copper systematics in arc magmas and implications for crust-mantle differentiation. Science 336:64–68
43. Lee C-T, Rudnick RL, Brimhall GH (2001) Deep lithospheric dynamics beneath the Sierra Nevada during the Mesozoic and Cenozoic as inferred from xenolith petrology. Geochem Geophys Geosys. doi:10.1029/2001GC000152
44. Manley CR, Glazner AF, Farmer GL (2000) Timing of volcanism in the Sierra Nevada of California: evidence for Pliocene delamination of the batholithic root? Geology 28:811–814
45. Farmer GL, Glazner AF, Manley CR (2002) Did lithospheric delamination trigger late Cenozoic potassic volcanism in the southern Sierra Nevada, California? Geol Soc Am Bull 114: 754–768
46. Müntener O, Kelemen PB, Grove TL (2001) The role of H_2O during crystallization of primitive arc magmas under uppermost mantle conditions and genesis of igneous pyroxenites: an experimental study. Contrib Mineral Petrol 141:643–658
47. Anderson DL (2005) Large igneous provinces, delamination, and fertile mantle. Elements 1:271–275
48. Pertermann M, Hirschmann MM (2003) Partial melting experiments on a MORB-like pyroxenite between 2 and 3 GPa: constraints on the presence of pyroxenites in basalt source regions. J Geophys Res 108:000111–000117. doi:10.1029/2000JB000118
49. Pertermann M, Hirschmann MM (2003) Anhydrous partial melting experiments on MORB-like eclogite: phase relations, phase compositions and mineral-melt partitioning of major elements at 2–3 GPa. J Petrol 44:2173–2201
50. Sisson TW, Grove TL, Coleman RG (1996) Hornblende gabbro sill complex at Onion valley, California, and a mixing origin for the Sierra Nevada batholith. Contrib Mineral Petrol 126:81–108
51. Alonso-Perez R, Müntener O, Ulmer P (2009) Igneous garnet and amphibole fractionation in the roots of island arcs: experimental constraints on andesitic liquids. Contrib Mineral Petrol 157:541–558
52. Lee C-TA, Lee T-C, Wu C-T (2014) Modeling the compositional evolution of recharging, evacuating, and fractionating (REFC) magma chambers: implications for differentiation of arc magmas. Geochim Cosmochim Acta 143:8–22
53. England P, Katz RF (2010) Melting above the anhydrous solidus controls the location of volcanic arcs. Nature 467:700–704
54. Karlstrom L, Lee C-TA, Manga M (2014) The role of magmatically driven lithospheric thickening on arc front migration. Geochem Geophys Geosys. doi:10.1002/2014GC005355
55. Lee C-TA (2003) Compositional variation of density and seismic velocities in natural peridotites at STP conditions: implications for seismic imaging of compositional heterogeneities in the upper mantle. J Geophys Res. doi:10.1029/2003JB002413
56. Arevalo R, McDonough WF (2010) Chemical variations and regional diversity observed in MORB. Chem Geol 271:70–85
57. Bird P (2003) An updated digital model of plate boundaries. Geochem Geophys Geosys. doi:10.1029/2001GC000252
58. Clift PD, Vannucchi P, Phipps Morgan J (2009) Crustal redistribution, crust-mantle recycling and Phanerozoic evolution of the continental crust. Earth-Sci Rev 97:80–104
59. Plank T, Langmuir C (1998) The chemical composition of subducting sediment and its consequences for the crust and mantle. Chem Geol 145:325–394
60. von Huene R, Scholl D (1991) Observations at convergent margins concerning sediment subduction, subduction erosion, and the growth of continental crust. Rev Geophys 29:279–316
61. Peacock SM (1990) Fluid processes in subduction zones. Science 248:329–337
62. Jicha BR, Scholl DW, Singer BS et al (2006) Revised age of Aleutian island arc formation implies high rate of magma production. Geology 34:661–664
63. Mukhopadhyay B, Manton WI (1994) Upper mantle fragments from beneath the Sierra Nevada batholith-partial fusion, fractional crystallization and metasomatism in subduction-related ancient lithosphere. J Petrol 35:1418–1450
64. Chin EJ, Lee C-TA, Barnes J (2014) Thickening, refertilization, and the deep lithosphere filter in continental arcs: constraints from major and trace elements and oxygen isotopes. Earth Planet Sci Lett 397:184–200
65. Chin EJ, Lee C-TA, Luffi P et al (2012) Deep lithospheric thickening and refertilization beneath continental arcs: case study of the P, T and compositional evolution of peridotite xenoliths from the Sierra Nevada, California. J Petrol 53: 477–511
66. Chin EJ, Lee C-TA, Blichert-Toft J (2015) Growth of upper plate lithosphere controls tempo of arc magmatism: constraints

from Al-diffusion kinetics and coupled Lu–Hf and Sm–Nd chronology. Geochem Perspect Lett 1:20–32
67. Ranalli G, Murphy DC (1987) Rheological stratification of the lithosphere. Tectonophysics 132:281–295
68. Gazel E, Plank T, Forsyth D et al (2012) Lithosphere versus asthenosphere mantle sources at the Big Pine volcanic field, California. Geochem Geophys Geosys. doi:10.1029/2012GC004060
69. Boyd OS, Jones CH, Sheehan AF (2004) Foundering lithosphere imaged beneath the southern Sierra Nevada, California, USA. Science 305:660–662
70. Saleeby J, Ducea M, Clemens-Knott D (2003) Production and loss of high-density batholithic root, southern Sierra Nevada, California. Tectonics. doi:10.1029/2002TC001374
71. Le Pourhiet L, Gurnis M, Saleeby J (2006) Mantle instability beneath the Sierra Nevada Mountains in California and Death Valley extension. Earth Planet Sci Lett 251:104–119
72. Elkins Tanton LT (2007) Continental magmatism, volatile recycling, and a heterogeneous mantle caused by lithospheric gravitational instabilities. J Geophys Res. doi:10.1029/2005JB004072
73. Behn M, Hirth G, Kelemen PB (2007) Trench-parallel anisotropy produced by foundering of arc lower crust. Science 317:1141108–1141111. doi:10.1126/science/1141269
74. Kohlstedt DL, Evans B, Mackwell SJ (1995) Strength of the lithosphere: constraints imposed by laboratory experiments. J Geophys Res 100:17587–17602
75. Bird RB, Armstrong RC, Hassager O (1987) Dynamics of polymeric liquids: fluid mechanics, vol 1. Wiley, London
76. Wang Y, Huang J, Zhong S (2015) Episodic and multistaged gravitational instability of cratonic lithosphere and its implications for reactivation of the North China Craton. Geochem Geophys Geosys. doi:10.1002/2014GC005681
77. Lenardic A, Moresi L-N, Muhlhaus H-B (2003) Longevity and stability of cratonic lithosphere: insights from numerical simulations of coupled mantle convection and continental tectonics. J Geophys Res. doi:10.1029/2002JB001859
78. Sleep NH (2004) Evolution of the continental lithosphere. Annu Rev Earth Planet Sci 33:369–393
79. Sleep NH (2003) Survival of Archean cratonal lithosphere. J Geophys Res. doi:10.1029/2001JB000169
80. Jaupart C, Molnar P, Cottrell E (2007) Instability of a chemically dense layer heated from below and overlain by a deep less viscous fluid. J Fluid Mech 572:433–469
81. Lee C-TA, Luffi P, Chin EJ (2011) Building and destroying continental mantle. Annu Rev Earth Planet Sci 39:59–90
82. Lee C-TA, Lenardic A, Cooper CM et al (2005) The role of chemical boundary layers in regulating the thickness of continental and oceanic thermal boundary layers. Earth Planet Sci Lett 230:379–395
83. Lee C-TA, Luffi P, Plank T et al (2009) Constraints on the depths and temperatures of basaltic magma generation on Earth and other terrestrial planets using new thermobarometers for mafic magmas. Earth Planet Sci Lett 279:20–33
84. Elkins Tanton LT, Grove TL, Donnelly-Nolan JM (2001) Hot, shallow mantle melting under the Cascades volcanic arc. Geology 29:631–634
85. Drummond MS, Defant MJ, Kepezhinskas PK (1996) Petrogenesis of slab-derived trondhjemite–tonalite–dacite/adakite magmas. Trans R Soc Edinb 87:205–215
86. Liu X-M, Rudnick RL (2011) Constraints on continental crustal mass loss via chemical weathering using lithium and its isotopes. Proc Natl Acad Sci USA 109:19873–19875
87. Lee C-TA, Morton DM, Little MG et al (2008) Regulating continent growth and composition by chemical weathering. Proc Natl Acad Sci USA 105:4981–4985
88. Hacker BR, Kelemen PB, Behn MD (2011) Differentiation of the continental crust by relamination. Earth Planet Sci Lett 307:501–516
89. Bateman PC, Clark LD, Huber NK, et al (1963) The Sierra Nevada batholith: a synthesis of recent work across the central part. In: US Geological Survey Professional Paper, vol 414-D, p 46
90. Lee C-T, Yin Q-Z, Rudnick RL et al (2000) Osmium isotopic evidence for Mesozoic removal of lithospheric mantle beneath the Sierra Nevada, California. Science 289:1912–1916
91. Haschke MR, Scheuber E, Günther D et al (2002) Evolutionary cycles during Andean orogeny: repeated slab breakoff and flat subduction? Terra Nova 14:49–55
92. DeCelles PG, Ducea MN, Kapp P et al (2009) Cyclicity in Cordilleran orogenic systems. Nat Geosci 2:251–257
93. Chin EJ, Lee C-TA, Tollstrup DL et al (2013) On the origin of hot metasedimentary quartzites in the lower crust of continental arcs. Earth Planet Sci Lett 361:120–133
94. Plank T, Langmuir CH (1988) An evaluation of the global variations in the major element chemistry of arc basalts. Earth Planet Sci Lett 90:349–370
95. Huang S, Lee C-TA, Yin Q-Z (2014) Missing lead and high $^{3}He/^{4}He$ in ancient sulfides associated with continental crust formation. Sci Rep. doi:10.1038/srep05314
96. Hofmann AW (1997) Mantle geochemistry: the message from oceanic volcanism. Nature 385:219–229
97. Hirschmann MM, Stolper E (1996) A possible role for garnet pyroxenite in the origin of the "garnet signature" in MORB. Contrib Mineral Petrol 124:185–208
98. Hirschmann MM (2000) The mantle solidus: experimental constraints and the effects of peridotite composition. Geochem Geophys Geosys 1:2000GC000070
99. Kogiso T, Hirschmann MM, Frost DJ (2003) High-pressure partial melting of garnet pyroxenite: possible mafic lithologies in the source of ocean island basalts. Earth Planet Sci Lett 216:603–617
100. Keshav S, Gudfinnsson GH, Sen G et al (2004) High-pressure melting experiments on garnet clinopyroxenite and the alkalic to tholeiitic transition in ocean-island basalts. Earth Planet Sci Lett 223:365–379
101. Dasgupta R, Jackson MG, Lee C-TA (2010) Major element chemistry of ocean island basalts—conditions of mantle melting and heterogeneity of mantle source. Earth Planet Sci Lett 289:377–392
102. Mallik A, Dasgupta R (2012) Reaction between MORB-eclogite derived melts and fertile peridotite and generation of ocean island basalts. Earth Planet Sci Lett 329–330:97–108
103. Herzberg C (2011) Identification of source lithology in the Hawaiian and Canary Islands: implications for origins. J Petrol 52:113–146
104. Le Roux V, Dasgupta R, Lee C-TA (2011) Mineralogical heterogeneities in the Earth's mantle: constraints from Mn Co, Ni and Zn partitioning during partial melting. Earth Planet Sci Lett 307:395–408
105. Le Roux V, Lee C-TA, Turner SJ (2010) Zn/Fe systematics in mafic and ultramafic systems: implications for detecting major element heterogeneities in the Earth's mantle. Geochim Cosmochim Acta 74:2779–2796
106. Liu Y, Gao S, Kelemen P et al (2008) Recycled crust controls contrasting source compositions of Mesozoic and Cenozoic basalts in the North China Craton. Geochim Cosmochim Acta 72:2349–2376
107. Sobolev AV, Hofmann AW, Sobolev SV et al (2005) An olivine-free mantle source of Hawaiian shield basalts. Nature 434:590–597
108. Leeman WP, Harry DL (1993) A binary source model for extension-related magmatism in the Great Basin, western North America. Science 262:1550–1554

109. Lee C-TA, Shen B, Slotnick BS et al (2013) Continental arc-island arc fluctuations, growth of crustal carbonates and long-term climate change. Geosphere 9:21–36
110. Jahn B-M, Wu FY, Chen B (2000) Massive granitoid generation in Central Asia: Nd isotope evidence and implication for continental growth in the Phanerozoic. Episodes 23:82–92
111. Bateman PC, Eaton JP (1967) The Sierra Nevada Batholith. Science 158:1407–1417
112. Li X, Qi C, Liu Y et al (2005) Petrogenesis of the Neoproterozoic bimodal volcanic rocks along the western margin of the Yangtze block: new constraints from Hf isotopes and Fe/Mn ratios. Chin Sci Bull 50:2481–2486
113. Zhang J-J, Zheng Y-F, Zhao Z-F (2009) Geochemical evidence for interaction between oceanic crust and lithospheric mantle in the origin of Cenozoic continental basalts in east-central China. Lithos 110:305–326
114. Zheng X, Zhao Z-F, Zheng Y-F (2012) Slab–mantle interaction for thinning of cratonic lithospheric mantle in north China: geochemical evidence from Cenozoic continental basalts in central Shandong. Lithos 146–147:202–217
115. Gao S, Rudnick RL, Yuan H-L et al (2004) Recycling lower continental crust in the North China Craton. Nature 432:03892–03897. doi:10.1038/nature03162
116. Liu Y, Shan G, Lee C-TA et al (2005) Melt-peridotite interactions: links between garnet pyroxenite and high-Mg# signature of continental crust. Earth Planet Sci Lett 234:39–57
117. Xu Y-G (2001) Thermo-tectonic destruction of the Archaean lithospheric keel beneath the Sino-Korean craton in China: evidence, timing and mechanism. Phys Chem Earth A: Solid Earth Geod 26:747–757
118. Menzies M, Xu Y, Zhang H (2007) Integration of geology, geophysics and geochemistry: a key to understanding the North China Craton. Lithos 96:1–21
119. Niu Y (2014) Geological understanding of plate tectonics: basic concepts, illustrations, examples and new perspectives. Glob Tecton Metal 10:23–46
120. Niu Y (2005) Generation and evolution of basaltic magmas: some basic concepts and a hypothesis for the origin of the Mesozoic–Cenozoic volcanism in eastern China. Geol J China Univ 11:9–46
121. Zheng JP, Lee C-TA, Lu JG et al (2015) Refertilization-driven destabilization of subcontinental mantle and the importance of initial lithospheric thickness for the fate of continents. Earth Planet Sci Lett 409:225–231
122. Lee C-T (2001) The origin, evolution, and demise of continental lithospheric mantle: perspectives from Re–Os isotopes, geochemistry, petrology, and modeling. Harvard University, PhD Thesis